Journal of Magnetism and Magnetic Materials 427 (2017) 114–121

Contents lists available at ScienceDirect

Journal of Magnetism and Magnetic Materials

journal homepage: www.elsevier.com/locate/jmmm

Preparation of poly-L-lysine functionalized magnetic nanoparticles and their influence on viability of cancer cells

I. Khmara[a,c], M. Koneracka[a], M. Kubovcikova[a], V. Zavisova[a,*], I. Antal[a], K. Csach[a], P. Kopcansky[a], I. Vidlickova[b], L. Csaderova[b], S. Pastorekova[b], M. Zatovicova[b]

[a] Institute of Experimental Physics, Slovak Academy of Sciences, Watsonova 47, Kosice, Slovakia
[b] Institute of Virology, Biomedical Research Center, Slovak Academy of Sciences, Dubravska cesta 9, Bratislava, Slovakia
[c] Pavol Jozef Safarik University, Faculty of Science, Park Angelinum 9, Kosice, Slovakia

ARTICLE INFO

Keywords:
Magnetic nanoparticles
Poly-L-lysine
Antibody
Carbonic anhydrase IX
Cancer detection

ABSTRACT

This study was aimed at development of biocompatible amino-functionalized magnetic nanoparticles as carriers of specific antibodies able to detect and/or target cancer cells. Poly-L-lysine (PLL)-modified magnetic nanoparticle samples with different PLL/Fe_3O_4 content were prepared and tested to define the optimal PLL/Fe_3O_4 weight ratio. The samples were characterized for particle size and morphology (SEM, TEM and DLS), and surface properties (zeta potential measurements). The optimal PLL/Fe_3O_4 weight ratio of 1.0 based on both zeta potential and DLS measurements was in agreement with the UV/VIS measurements. Magnetic nanoparticles with the optimal PLL content were conjugated with antibody specific for the cancer biomarker carbonic anhydrase IX (CA IX), which is induced by hypoxia, a physiologic stress present in solid tumors and linked with aggressive tumor behavior. CA IX is localized on the cell surface with the antibody-binding epitope facing the extracellular space and is therefore suitable for antibody-based targeting of tumor cells. Here we showed that PLL/Fe_3O_4 magnetic nanoparticles exhibit cytotoxic activities in a cell type-dependent manner and bind to cells expressing CA IX when conjugated with the CA IX-specific antibody. These data support further investigations of the CA IX antibody-conjugated, magnetic field-guided/activated nanoparticles as tools in anticancer strategies.

1. Introduction

Recent advances in understanding mechanisms of cancer development and progression have facilitated development of new treatment modalities, strategies for patients' stratification and identification of novel promising molecular targets. The development of targeted therapy has now become more tailored to the individual patient and to specific tumor types. Personalized treatment can reduce side effects associated with current nonspecific cancer therapies. Sensitive tumor detection and effective targeted therapy are two important challenges in successful treatment of cancer patients.

Thus, combinations of the molecular approaches with new nanotechnologies and materials offer new opportunities for improvements of cancer therapy. Magnetic nanoparticles (MNPs) possess unique properties that make them highly attractive to medical applications.

The applicability of magnetic fluids (MFs) containing MNPs requires special properties of particles such as superparamagnetic behavior at room temperature, colloidal stability [1], which depends on the size of the MNPs and biocompatibility of polymer coating [2,3], respectively. Coating of the MNPs by biocompatible polymers (such as dextran or protein) [4] makes it possible to prevent the formation of large aggregates and to restrain the biodegradation caused by the influence of biological systems. The surface of the polymer also has adsorbing ability mediated by covalent attachments [5]. Excellent properties of magnetic fluids predispose them for diagnostic and therapeutic applications [6], e.g. as contrast agents for magnetic resonance imaging, for local magnetic hyperthermia treatment, or for targeted drug delivery with the potential use in oncology. Due to their properties, MNPs can be located at any desired place by localized magnetic field gradients, kept in place for as long as required by the particular therapy process, and consequently removed from the body [7].

These aspects of the MNPs utilization are undoubtedly highly positive, however, it is necessary to choose the optimal method of the synthesis of nanomaterials that determines the shape, size, and surface chemistry of the particles, and hence their magnetic properties.

* Corresponding author.
E-mail address: zavisova@saske.sk (V. Zavisova).

http://dx.doi.org/10.1016/j.jmmm.2016.11.014
Received 24 June 2016; Received in revised form 24 October 2016; Accepted 1 November 2016
Available online 05 November 2016
0304-8853/

Moreover, most of these applications require well-dispersed biocompatible particles. One of the effective ways to prevent particle agglomeration and confer biocompatibility is coating of nanoparticles with polymers and/or other targeting agents.

Biocompatible Poly-L-Lysine (PLL), is a synthetic polymer composed of the positively charged amino acid lysine that is widely used in the pharmaceutical industry. Its sub-products, monomeric amino acid lysine units, are characterized by no toxicity, no antigenicity, good biocompatibility and biodegradability [8].

In this paper we focused on detection and targeting of tumor cells using an antibody coupled to MNPs. Solid tumors are often hypoxic, because the growing tumor mass is inefficiently vascularized by aberrant blood vessels, which fail to deliver sufficient amount of oxygen to certain tumor tissue areas. It has been well documented that hypoxic tumors are more metastatic and resistant to chemo/radiotherapy [9]. Therefore, targeting hypoxic tumor cells can be achieved through hypoxia-induced molecules. Carbonic anhydrase IX (CA IX) is one of the best intrinsic markers of tumor hypoxia due to its very strong induction by low oxygen expressed in different types of solid tumors and is frequently associated with aggressive tumor phenotype [10]. Here we show that CA IX specific antibody coupled to MNPs can be used for selective detection of the CA IX-positive cancer cell lines. For this purpose, we employed our highly specific monoclonal antibody M75 binding to the extracellular domain of CA IX. The antibody was coupled to nanoparticles and utilized for targeting of the CA IX-expressing cells.

2. Materials and methods

2.1. Materials

Poly-L-Lysine (PLL, molecular weight Mw =150 000–300 000), ferric chloride hexahydrate ($FeCl_3 \cdot 6H_2O$), ferrous sulphate heptahydrate ($FeSO_4 \cdot 7H_2O$), and ammonium hydroxide (NH_4OH) were purchased from Sigma-Aldrich. All solutions were prepared using an ultrapurified water. Human CA IX PG domain-specific mouse monoclonal antibody M75 was described previously [11].

2.1.1. Cell culture

For the experiments described in this paper, we used human cervical cancer cells C33a permanently transfected with the full-length CA9 cDNA in pcDNA3.1+ plasmid (C33 CA IX). Mock-transfected cells (C33 neo) were used as a negative control. We also used MDCK canine kidney cells permanently transfected with the full-length human carbonic anhydrase (CA9) cDNA in the pSG5C plasmid (MDCK CA IX). Mock-transfected cells (MDCK neo) were used as a negative control. Human tumor-derived cell lines with endogenous CA IX expression, such as cervical carcinoma HeLa cells, colon carcinoma RKO cells, renal carcinoma ACHN *cells,* lung adenocarcinoma A549 cells*, as well as CA IX-negative HEK 293* human embryonic kidney cells, MRC5 human lung (fetal) fibroblast, NIH 3T3 mouse embryonic fibroblast cell line, CHO Chinese hamster ovary cells and BHK baby hamster kidney fibroblasts were used for in vitro experiments. The cells were routinely cultivated in DMEM medium with 10% FCS (BioWhittaker) at 37 °C in 5% CO_2 in air.

2.2. Synthesis of Fe_3O_4 MNPs and their surface modification with PLL

Magnetic fluids containing magnetic nanoparticles modified by PLL (MFPLLs) were prepared as follows. First, magnetite nanoparticles were formed by precipitation of Fe(2+) and Fe(3+) ions in aqueous solution with a dropwise addition of ammonium hydroxide. The black precipitate was washed 4 times and put in a glass vial with defined volume of water. Then, the ultrasonication was applied using an immersed probe (horn tip) of a sonicator (BRANSON - Model 450) for 5 min at 70% of maximum power (280 W) in the water bath. In the next step, a modification of magnetite nanoparticles with PLL was done. The suspension of nanoparticles was mixed with Poly-L-Lysine solution (0.1%) at the theoretical PLL/Fe_3O_4 weight ratio from 0.1 to 3.9 (corresponding to PLL loading 0.02–0.9 mg/mL). The mixture was sonicated for 5 min at 70% power in the ice bath. Consequently, the samples were subjected to ultracentrifugation at 44,000*g* for 2 h at 4 °C in order to increase their concentration. Then the supernatants were removed and the sediments were thoroughly dispersed in ultrapure water and collected. By this procedure, the MFPLLs with the PLL/Fe_3O_4 weight ratio values from 0.1 to 3.9 were obtained.

2.3. Antibody conjugation to MFPLLs

Binding of the antibodies to amino-modified MFPLL was carried out using the carbodiimide procedure described elsewhere [12]. The coupling reaction was conducted under different sets of condition to determine the optimum conditions for the antibody (Ab) immobilization. To study the effect of various MNPs to Ab ratios on the Ab immobilization, the reaction was carried out at pH 7 using 1 mM carbodiimide in PBS at constant weight ratio of carbodiimide (CDI) to Ab, whereas the ratio between MNPs and Ab varied from 1 to 5. Shortly, the reaction mixtures containing Ab, CDI and MFPLL were stirred 24 h at room temperature. Then the samples were centrifuged at 32,000*g* for 1 h at 4 °C and the amount of unbound Ab in the supernatant was estimated by Bradford's dye binding methods [13]. For each studied sample a corresponding blank comparative sample with no MNPs was prepared. Each sample with one of the ratios mentioned above was prepared in triplets.

2.4. Cell viability assay

To assess the toxicity of different nanoparticles and PLL on various cell lines, the Cell Titer Blue viability assay (Promega Madison, WI) was used. The assay was performed according to the manufacturer's instructions. Briefly, the cells were plated in 96-well plates (at 2000 cells/well, and at 10000 cells/well for MRC5) and allowed to grow for 24 h. MNPs were suspended in the culture medium at different concentrations (100, 50 and 10 μg/mL) and added to wells. The cells cultured in the medium without nanoparticles served as controls. After 24 h, 48 h and 5/6 days incubation, 20 μl of the Cell Titer Blue solution was directly added to the wells and incubated for 4 h at 37 °C. The fluorescence was recorded with 530 nm/590 nm (excitation/emission) filter set using Bio-Tek Synergy HT microplate reader. The samples were run in triplicates for each concentration of nanoparticles.

2.5. Immunofluorescence assay

Cells grown on glass coverslips were gently washed with PBS and fixed in ice-cold methanol at −20 °C for 5 min. Nonspecific binding was blocked by incubation with PBS containing 1% BSA for 30 min at 37 °C. Then, the cells were incubated with the free M75 antibody (5 μg/mL), M75 (5 μg/mL) conjugated to MNPs or with MFPLL without conjugated antibody diluted in 1% BSA in PBS for 1 h at 37 °C followed by an anti-mouse ALEXA 488–conjugated antibody (Invitrogen) diluted 1:1000 in the blocking buffer for 1 h at 37 °C to detect the M75 antibody. The nuclei were stained with DAPI (Sigma). Finally, the coverslips were mounted onto slides in the Fluorescent Mounting Media (Sigma), and analyzed by the confocal laser scanning microscope Zeiss LSM 510 Meta.

2.5.1. Immunofluorescence-based internalization assay

The immunofluorescence-based internalization assay was performed using the established MDCK cell model. MDCK CA IX cells (700 000 cells per Petri dish) were plated on sterile glass coverslips 24 h before the experiment. Subsequently the live cells were incubated with the free M75 antibody (5 μg/mL) or the M75 (5 μg/mL) con-

jugated to MNPs, each diluted in culture medium, for 3 h at 37 °C to allow for the internalization of the CA IX-bound M75 antibody or the M75-conjugated MFPLL. At the end of the internalization period, the cells were thoroughly washed to remove the unbound antibody. Presence of the M75 Ab was visualized in the cells fixed in ice-cold methanol at −20 °C for 5 min using the anti-mouse ALEXA 488-conjugated secondary antibody. Finally, the cells were mounted onto slides and analyzed by the confocal laser-scanning microscope Zeiss LSM 510 Meta.

2.6. Characterization of Fe_3O_4 and PLL-modified MNPs

Transmission electron microscopy (TEM) analysis was performed using the JEOL-TEM 2100 F microscope operated at 200 kV. Scanning electron microscopy (SEM, JEOL7000F microscope) was used to evaluate the morphology and microstructure of the coated nanoparticles in the prepared samples. To determine the particle size distribution, the samples were measured by Dynamic light scattering (DLS) using Zetasizer NanoZS (Malvern Instruments). The zeta potential was estimated using a Laser Doppler Electrophoretic measurement technique with a scattering angle of 173° at 25 ± 0.1 °C. DLS evaluates the fluctuations of scattered light intensity diffracted from nanoparticles undergoing the steady Brownian motion in suspension.

3. Results and discussion

Magnetic fluid containing magnetic nanoparticles stabilized by PLL with different PLL/Fe_3O_4 ratios were prepared and characterized by various techniques. X-ray diffraction (XRD) technique was used for the qualification of magnetite. The nanoparticles synthesized by the co-precipitation method were proven to consist of magnetite as the six peaks corresponding to magnetite, namely of Miller indices {220}, {311}, {400}, {422}, {511, 333}, and {440} were present in the samples [14]. TEM microscopy was applied to study the morphology and shape of the nanoparticles. Magnetic cores of the uncoated and PLL-modified magnetic nanoparticles were roughly spherical with the diameter of approximately 7–15 nm, as shown by TEM (Fig. 1a, b). PLL modification significantly affected neither the morphology nor the size of the magnetic nanoparticles. Next, the PLL-modified magnetic nanoparticles were characterized by the SEM microscopy. The SEM image (Fig. 1c) revealed that the coated nanoparticles are spherical in shape with smooth surfaces and approximately of 90 nm in diameter.

To determine the efficiency of the PLL-adsorption on MNPs, a set of 11 samples was prepared and examined as a function of the initial amount of the PLL loading, which ranged from 0.05 to 0.8 mg/mL, while the amount of magnetite was kept constant (0.252 mg/mL Fe_3O_4). For the PLL estimation, the amount of the free amino acid

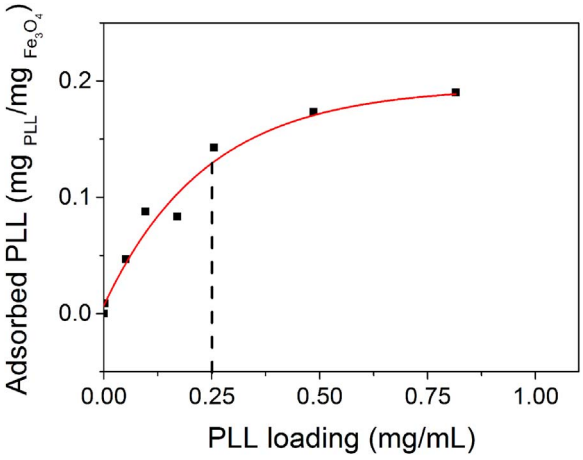

Fig. 2. Adsorption isotherm of PLL on MNPs.

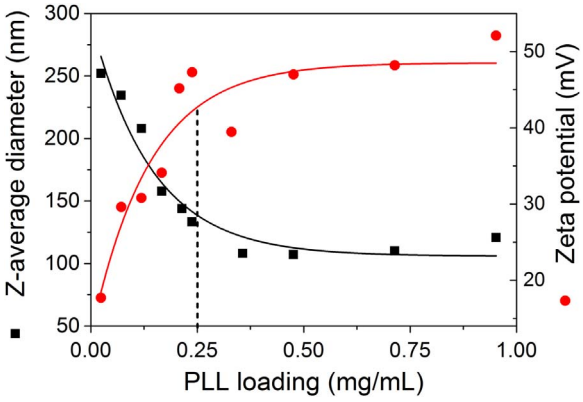

Fig. 3. Effects of various theoretical PLL loadings with regard to Z–average diameter and zeta potential.

present in the supernatant after MNPs centrifugation was determined by the UV spectrophotometer [15]. Briefly, the PLL concentration was estimated by the colorimetric determination using the trypan blue dye, which is precipitated quantitatively with polycations. Trypan blue solution was added to the sample of MFPLL. After a thorough mixing, the sample was incubated in thermomixer at 37 °C for 60 min and then centrifuged for 10 min at 4000 rpm. The supernatants from each of the test tubes were withdrawn and their absorbance at 580 nm was measured in UV/VIS spectrophotometer against the PBS without trypan blue (as a reference). The absorbance of the blank prepared by mixing PBS with trypan blue was set as 100%. The absorbance of an

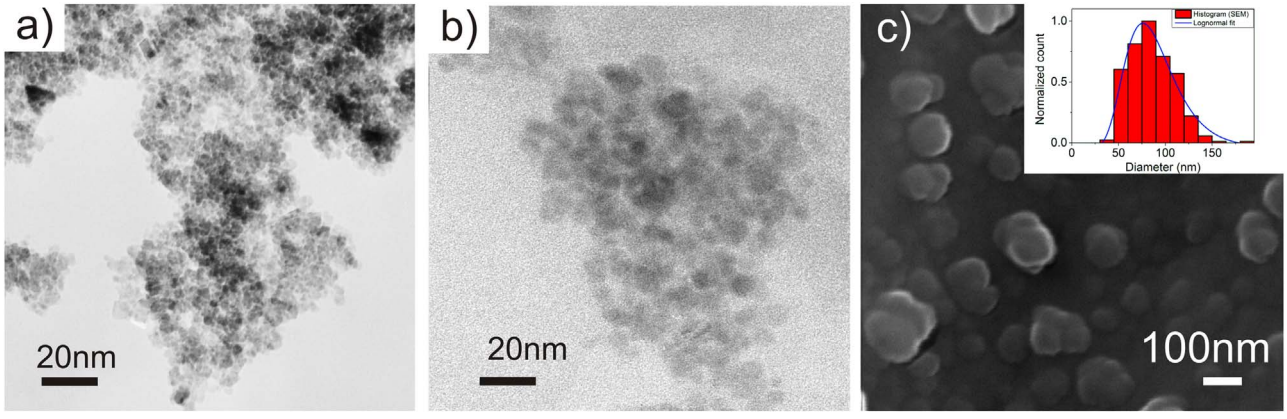

Fig. 1. TEM images of uncoated nanoparticles (a), PLL coated nanoparticles (weight ratio PLL/ Fe_3O_4 =1) (b), SEM image of PLL coated nanoparticles (PLL/ Fe_3O_4 =1) (c), and size distribution of PLL coated nanoparticles obtained from SEM (inset).

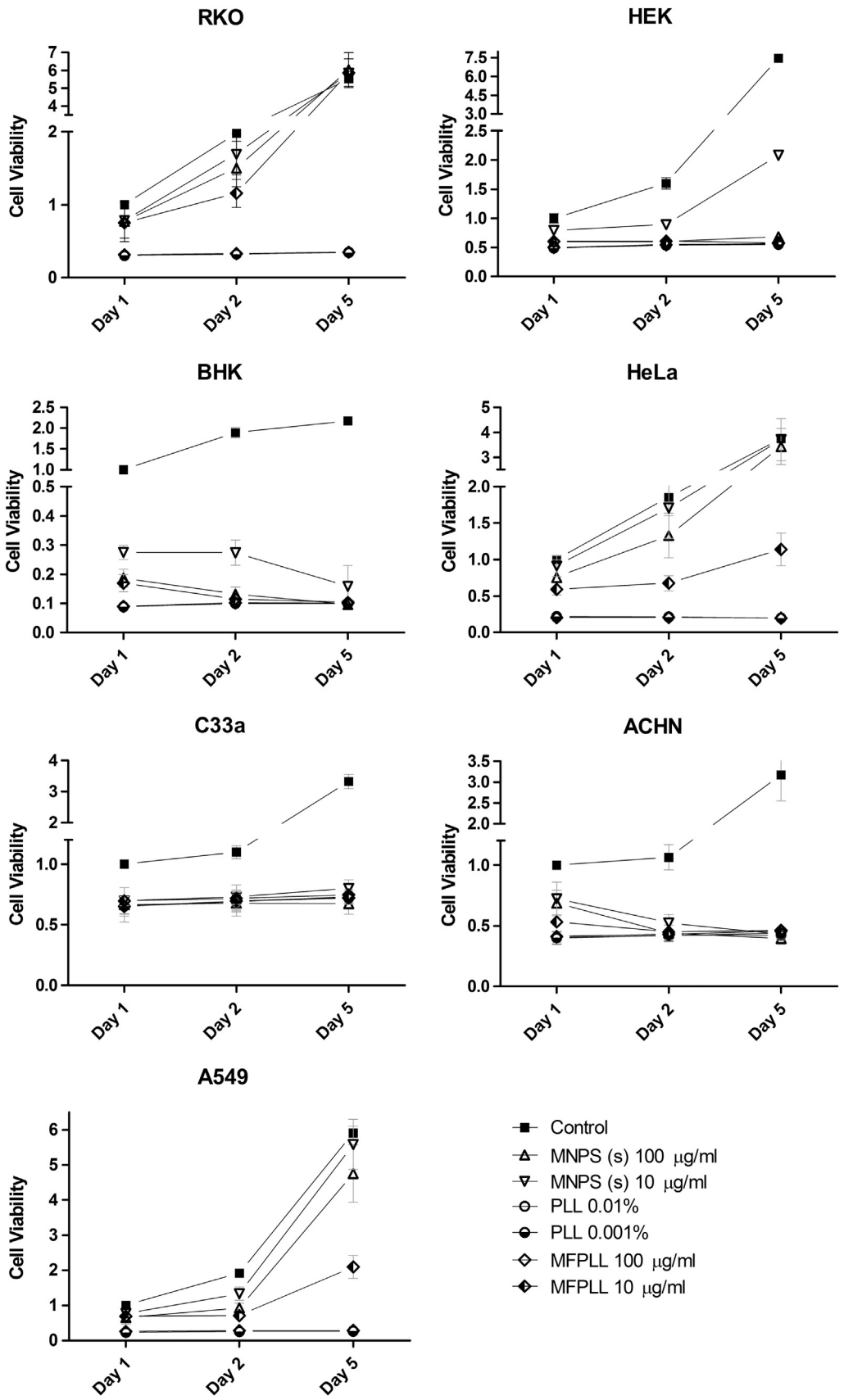

Fig. 4. Effect of MNPs, PLL, and MFPLL on the cell viability of various cancer and normal cell lines at various periods of incubation. Cell viability was measured by Cell Titer Blue assay and all values were normalized to the value of the control measured at day 1 (The viability of the control cells measured at the first day was set as 1). Each cell line was evaluated separately, and the viability values of treated cells were normalized to their corresponding control. Data in the graphs represent mean ± standard deviation values, all experiments were performed in triplicates.

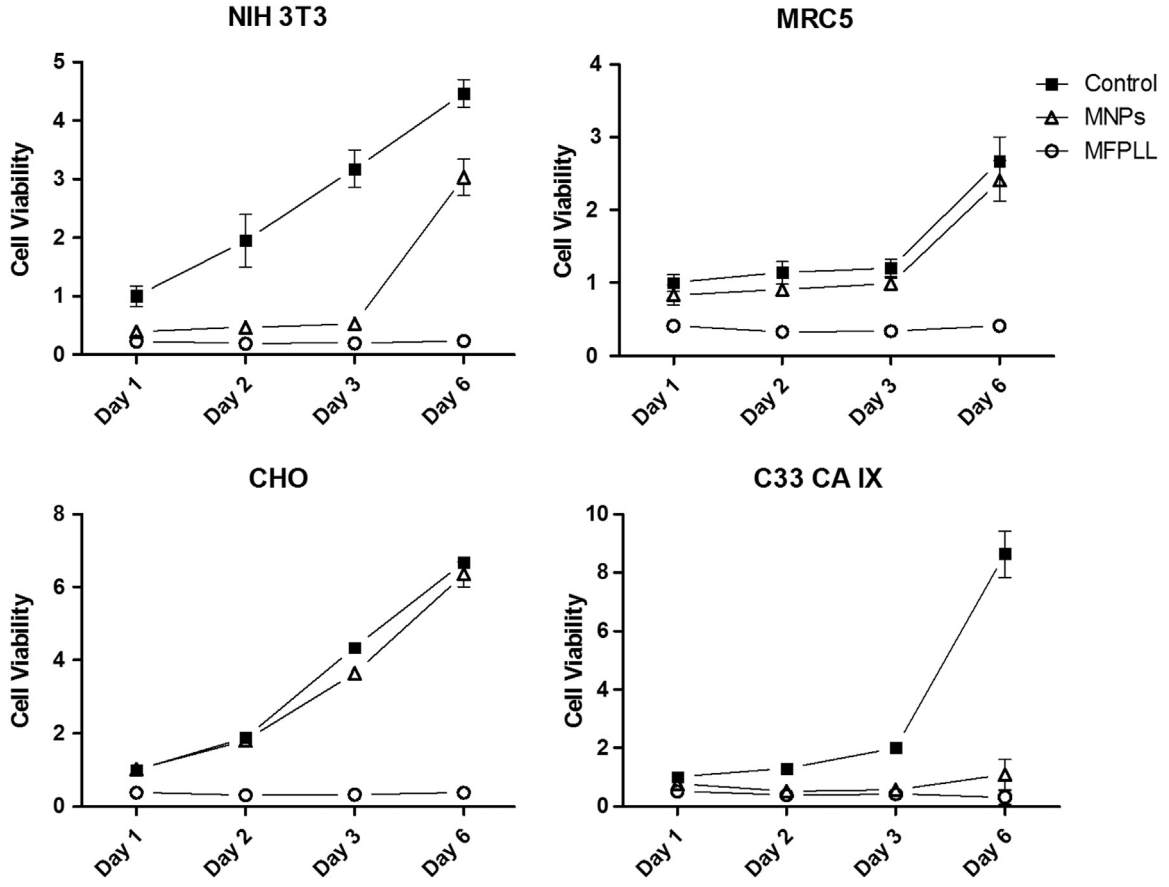

Fig. 5. Effect of MNPs and MFPLL on the cell viability of normal cells compared to CA IX expressing cancer cells at various periods of incubation. All viability values were normalized to the value of the control measured at day 1. Data in the graphs represent mean ± standard deviation values. Concentration of all types of magnetic nanoparticles was 50 μg/mL.

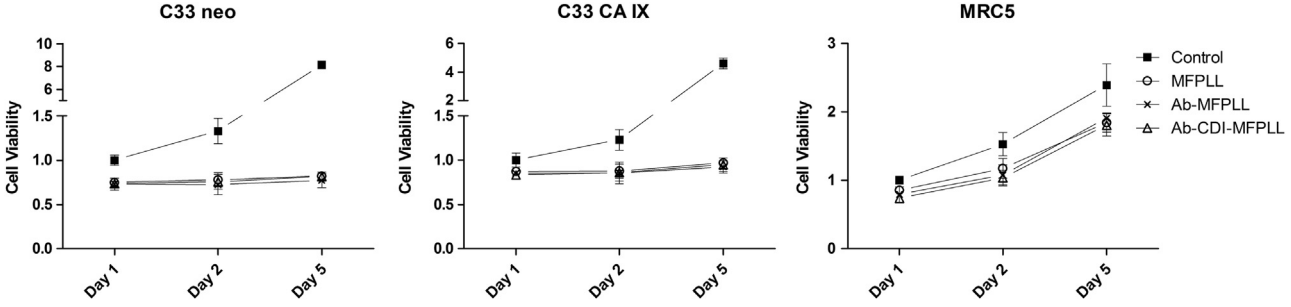

Fig. 6. Effect of Ab-MFPLL, Ab-CDI-MFPLL and MFPLL on the viability of C33 cancer cells expressing CA IX, control C33 neo cancer cells and normal MRC5 cells at various incubation periods. Data in the graphs represent mean ± standard deviation values. Concentration of conjugated antibody was 5 μg/mL and corresponding concentration of nanoparticles in all samples was 25 μg/mL.

unbound dye in the supernatant is inversely proportional to the concentration of this polyamino acid.

As shown on Fig. 2, the amount of adsorbed PLL increased with the PLL loading concentration, as calculated using the following mass balance equation:

Adsorbed PLL $=(C_o - C_e)$. V/m.

where *Co* and *Ce* are the initial and equilibrium concentrations of PLL solutions (mg/L), *V* is the solution volume (mL), and *m* is the adsorbent weight (in our case Fe_3O_4 in mg). Having fitted the experimental data, the optimal value of the PLL loading was found to be 0.25 mg/mL, which corresponds to the PLL/Fe_3O_4 weight ratio of 1.0.

Fig. 3 shows the effect of the PLL coating on the size of the MNPs. Based on the DLS analysis the mean particle diameter of the uncoated MNPs was observed to be 247 nm with the PDI =0.34, indicating that the uncoated nanoparticles aggregated. In the case of the coated nanoparticles (MFPLL), the hydrodynamic diameter decreased to the size of around 105 nm due to the PLL coating that avoided the aggregation of nanoparticles. This is supported also by the lower PDI of the coated nanoparticles (see the Suppl. Fig. 1). The stable value of the particle size was found to be 133 nm at the theoretical PLL/Fe_3O_4 weight ratio of 1 w/w, corresponding to the PLL loading concentration of 0.25 mg/mL. This optimal value of the PLL loading was also confirmed by the relationship of theoretical PLL loading versus PLL entrapment (Suppl. Fig. 2). The effect of the PLL adsorption on zeta potential value of samples was also investigated. Zeta potential of the uncoated MNPs was 18 mV, whereas the zeta potential of MFPLL was growing with the increasing PLL concentration until the plateau was reached at the value of approximately 50 mV. It is interesting that the shape of the adsorption curve (Fig. 2) was similar to the zeta potential curve profile and hydrodynamic diameter curve (Fig. 3), suggesting the correlation between the amount of adsorbed PLL and the stability of

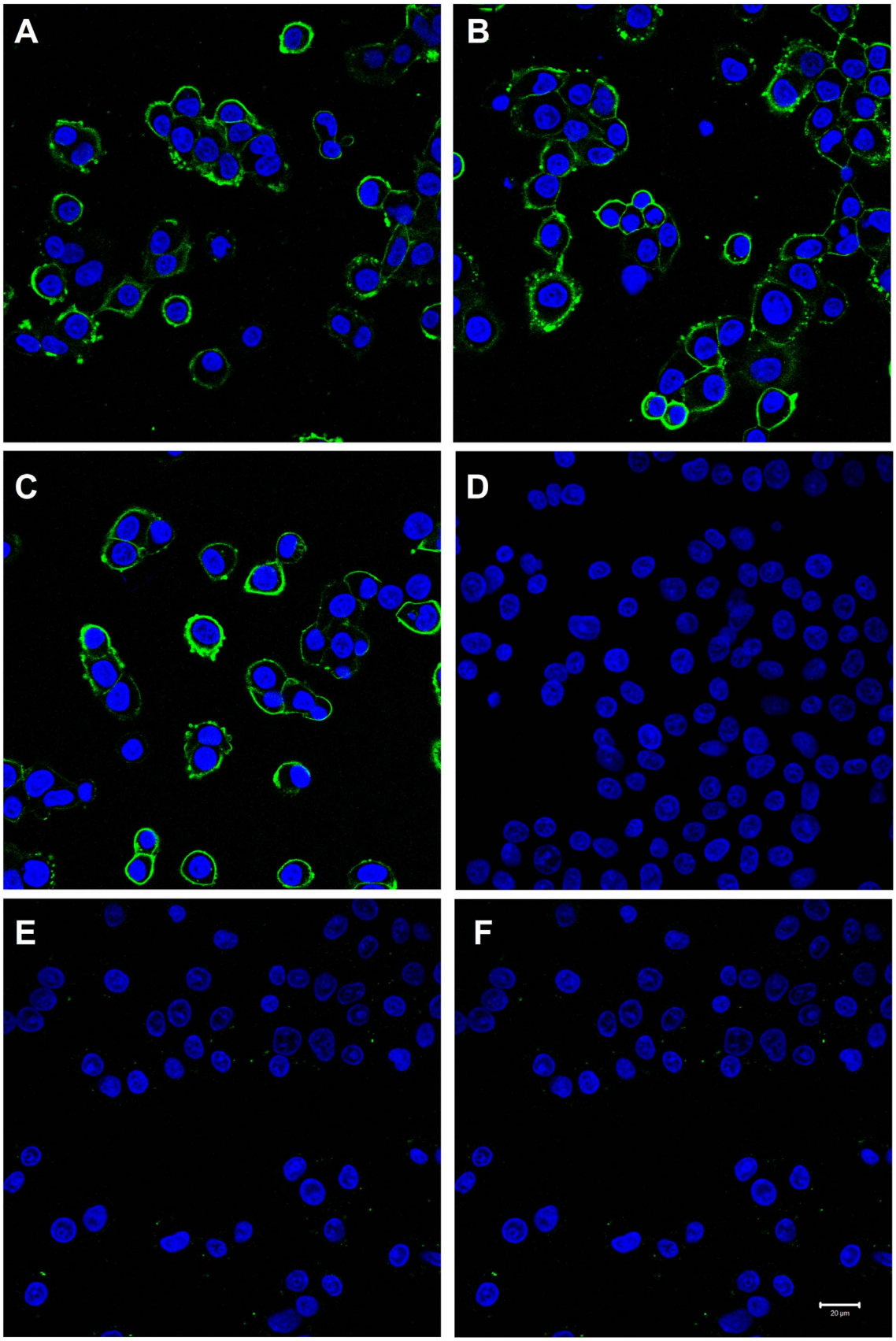

Fig. 7. Immunofluorescence detection of Ab-MFPLL (A) and Ab-CDI-MFPLL (B) binding to CA IX expressed in the plasma membranes of the transfected C33 CA IX cells. M75 antibody alone was used as a positive control (C). MFPLL nanoparticles without conjugated antibody did not bind to the CA IX expressing cells (D). Ab-MFPLL (E) and Ab-CDI-MFPLL (F) did not bind to control C33 neo cells lacking the CA IX protein. Scale bar 20 µm.

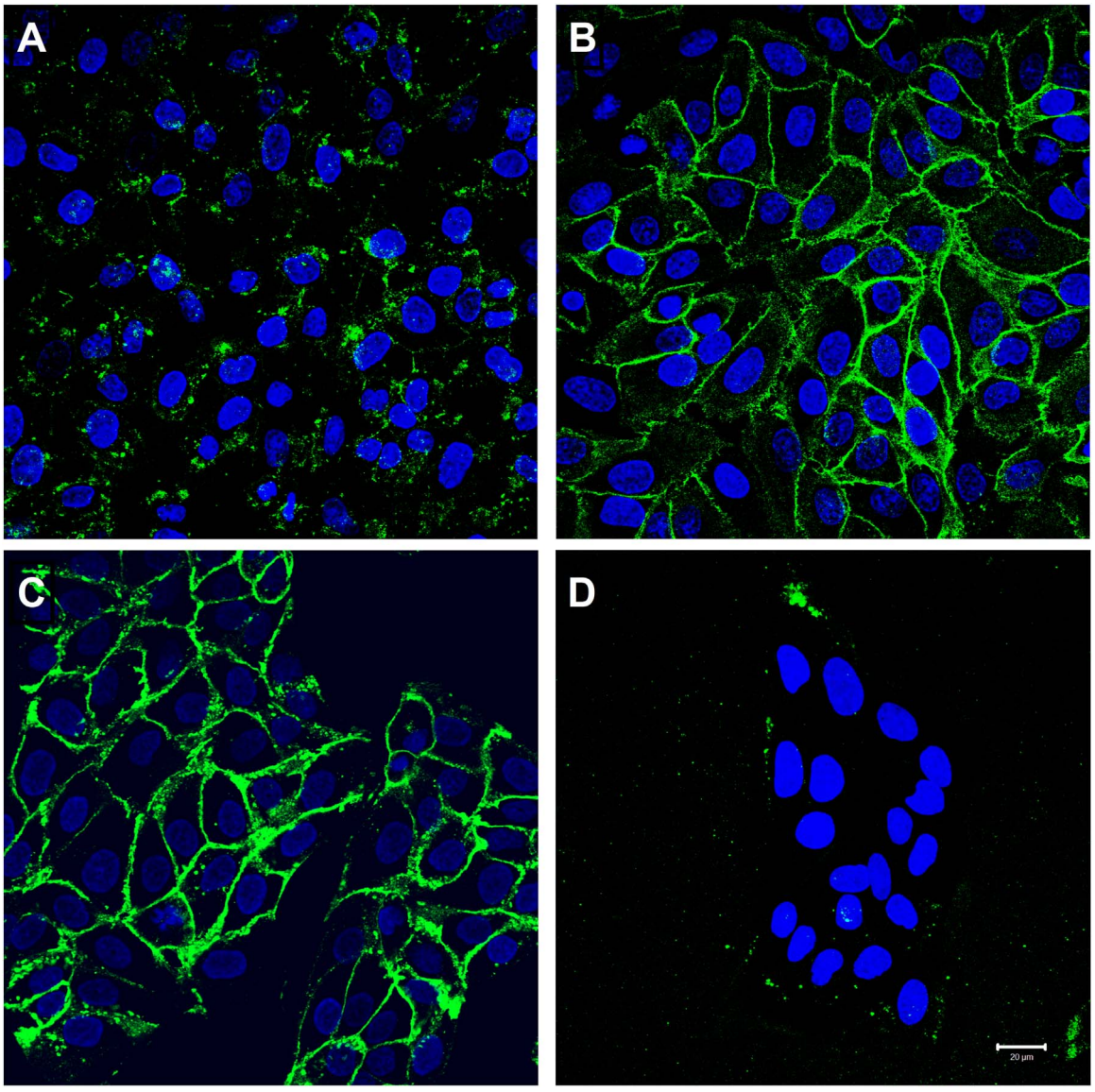

Fig. 8. Analysis of the M75 Ab-CDI-MFPLL nanoparticles for the capacity to internalize. MDCK CA IX cells grown on glass coverslips were incubated with Ab-CDI-MFPLL (containing 5 µg/mL conjugated antibody) at 37 °C to allow internalization (A) or 4 °C, when internalization is blocked, (B) for 3 h, washed and fixed with methanol. After incubation with the anti-mouse Alexa 488-conjugated secondary antibody for 1 h at 37 °C and washing, the cells were analyzed by confocal laser-scanning microscope Zeiss LSM 510 Meta. Z-stacks were acquired across the whole cell thickness and the overall antibody signal was evaluated by creating the projection image. The projection accumulates the positive signal from all z-stack planes, i.e. from the whole cell volume, and displays it in a single plane image. Only the M75 Ab conjugated to MFPLL showed punctuated intracellular staining signal indicating internalization. Free M75 antibody was unable to internalize at 37 °C and remained on the cell surface (C). Ab-CDI-MFPLL did not bind to MDCK neo cells that were used as a negative control (D). Scale bar 20 µm.

the nanoparticles.

As the key purpose of this study was to conjugate antibodies onto amino modified MNPs to utilize them subsequently for detection and treatment of cancer cells, we prepared the MFPLL with the PLL/Fe_3O_4 theoretical weight ratio of 1 w/w. After removal of the free PLL molecules, the sample contained 16 mg Fe_3O_4/mL and 3.1 mg PLL/mL. Immobilization of the Ab using the direct binding procedure showed that the extent of the Ab coating on the MNPs varied from 20% to 80%, corresponding to the MNPs/Ab ratio ranging from 1 to 5. The formulations of the Ab-MFPLL and Ab-CDI-MFPLL with the MNPs/Ab weight ratio of 5/1 were purified from the unbound Ab by washing and centrifugation at 22,000 rpm for 1 h at 4 °C. The resulting samples were selected as the optimal starting formulations for the cell culture studies.

First, cell viability was assayed to estimate cytostatic or cytotoxic properties of the MNP, MFPLL and PLL samples quantitatively by the cell titer blue method (CTT) (Fig. 4), in which the formation of resorufin fluorescent dye depends on the metabolic activity of the viable cells and reflects both proliferation-related increase and death-related decrease in the number of viable cells. The effect of MNPs (10 and 100 µg/mL) and PLL (0.01% and 0.001%) on various cell lines was observed after 24 h, 48 h and 5 days' exposure. Overall, the viability loss was dose- and time-related. The Fig. 4 clearly shows that some cell lines, namely RKO, HeLa and A549 survive and even proliferate in the presence of MNPS, while PLL and MFPLL appear to exhibit cytostatic effect. HEK cells display a reduced metabolism (i.e. viability) also with the lower concentration of MNPs. On the other hand, all treatments were cytostatic for C33a cells and even cytotoxic for ACHN and BHK cells, as demonstrated by a decreased trend of the viability values over time.

The cytotoxicity of MFPLL and MNPs (50 µg/mL) was also assessed using non-cancerous cell lines (Fig. 5) including NIH 3T3 mouse fibroblasts, CHO hamster ovary cells and MRC5 human embryonic fibroblasts in comparison to cancer cell line C33a stably transfected

with CA IX. In the conventional viability assay the cells exposed to nanoparticles exhibited differential cytostatic responses. MNPs showed good biocompatibility with MRC5 and CHO cells independently of the time exposure. The viability of C33 CA IX cancer cells was found to decrease with increasing time of the exposure to MNPs. However, MFPLL treatment resulted in the loss of viability observed in all cell lines.

In order to evaluate the cytotoxicity of the antibody-conjugated MNPs without CDI (Ab-MFPLL) and with the CDI coupling agent (Ab-CDI-MFPLL) in comparison with the antibody-free MFPLL, we analyzed the effects of these materials on the transfected C33 CA IX cells, control C33 neo cancer cells and normal MRC5 human fibroblasts (Fig. 6). All types of particles were cytostatic for both C33 neo and C33 CA IX cells, but only marginally reduced the proliferation of MRC5 cells, suggesting that their effect is cell type-specific.

Indirect immunofluorescence demonstrated that the M75 Ab-coupled MNPs, i.e. Ab-MFPLL and Ab-CDI-MFPLL (containing 5 μg/mL of coupled antibody) bound specifically to the CA IX antigen localized at the cell surface of the transfected C33 CA IX cells (Fig. 7 A, B) but not to the CA IX-negative C33 neo cells (Fig. 7 E, F). The distribution of the staining signal was identical to the distribution of the CA IX protein visualized by the antibody itself (Fig. 7 C). MFPLL nanoparticles without the conjugated antibody were used as a negative control (Fig. 7 D).

To prove that the observed staining signal was due to the M75 antibody-coupled nanoparticles interacting with the CA IX protein on the cell surface and not due to the free M75 antibody bound to CA IX, we performed additional experiment, in which we induced an internalization of the complex between CA IX and Ab-MNPs versus Ab alone (Fig. 8). This experiment was accomplished using the transfected MDCK CA IX cells as a model. The free M75 antibody could bind to the CA IX antigen exposed on the cell surface, but could not internalize at 37 °C. On the other hand, the M75 Ab coupled to CDI-MFPLL was capable of efficient internalization at 37 °C as demonstrated by the strong dotted intracellular immunofluorescence signal generated in the fixed cells by the secondary Alexa 488-conjugated anti-mouse antibody (Fig. 8A). This finding supports the view that the M75 Ab remains conjugated to nanoparticles, which mediate its uptake and intracellular accumulation and that the Ab-MNPs can be potentially used for the specific detection of the CA IX-expressing cells as well as also for the specific delivery and incorporation of nanoparticles into the cells.

4. Conclusion

Here we report the synthesis and detailed characterization of the amino functionalized MNPs. By tuning the PLL/Fe_3O_4 weight ratio, we were able to adjust the number of surface amino groups. The optimal content of the PLL was determined on the basis of zeta potential and UV/VIS measurements. Spherical shape of the nanoparticles was confirmed by electron microscopy. Hydrodynamic nanoparticle diameter, ranging from 100 to 200 nm in dependence on PLL/Fe_3O_4 weight ratio, was obtained by means of DLS measurement.

MNPs functionalized with PLL showed concentration- and time-dependent cytostatic or cytotoxic effects in a cell type-specific manner. Interestingly, high toxicity of the free PLL was reduced when PLL was conjugated to MNPs coupled with the antibody, probably due to the reduction of the overall PLL charge and/or due to selective delivery to cells expressing the target molecule. Cell-specific cytotoxicity could have been caused by differential ability of cells to accomplish internalization of MNPs that was previously shown to be associated with an increased production of reactive oxygen species as a stress response contributing to cell death [16]. Moreover, various cell types differ by their growth and division rate and it is well known that highly proliferating cells are more vulnerable to cytotoxic drugs or materials. Therefore, both of these conditions should be taken into account when designing optimal treatment of cells with MNPs to achieve cancer-selective effects. Moreover, these phenomena should be examined in 3D model of MNP accumulation and cytotoxicity in tumor spheroids to better predict selectivity and toxicity in vivo.

In conclusion, the specific binding to CA IX target molecule and intracellular accumulation of the Ab-MNPs in the CA IX-expressing cells generate key prerequisites for the selective detection and killing of cancer cells with high CA IX levels. Nevertheless, further extensive experimentation with magnetic field-guided and activated Ab-MNPs (associated with hyperthermia) is needed to prove this assumption.

Acknowledgments

This work was supported by the Slovak Research and Development Agency under the contracts No. APVV-14–0120 and APVV-14–0932, by COST TD 1402 Radiomag, by the Ministry of Education Agency for Structural Funds of EU (Project ITMS 26220220005), by the Slovak Scientific Grant Agency projects VEGA 2/0045/13, VEGA 2/0108/16 and VEGA 2/0081/14. I. Antal acknowledges the support of the National Scholarship Program for the Support of Mobility (SAIA), for an opportunity to stay and work at the Institute of Experimental Physics SAS in Kosice (Slovakia).

Appendix A. Supplementary material

Supplementary data associated with this article can be found in the online version at http://dx.doi.org/10.1016/j.jmmm.2016.11.014.

References

[1] P. Tartaj, M. del Puerto Morales, S. Veintemillas-Verdaguer, T. González-Carreño, C.J. Serna, The preparation of magnetic nanoparticles for applications in biomedicine, J. Phys. D: Appl. Phys. 36 (2003) R182–R197.
[2] M. Chanana, Z.W. Mao, D.Y. Wang, Using polymers to make up magnetic nanoparticles for biomedicine, J. Biomed. Nanotechnol. 5 (2009) 652–668.
[3] S.I. Park, J.H. Lim, J.H. Kim, H.I. Yun, J.S. Roh, C.G. Kim, C.O. Kim, Effects of surfactant on properties of magnetic fluids for biomedical application, Phys. Status Solidi B 241 (2004) 1662–1664.
[4] C.C. Berry, S. Wells, S. Charles, A.S.G. Curtis, Dextran and albumin derivatised iron oxide nanoparticles: influence on fibroblasts in vitro, Biomaterials 24 (2003) 4551–4557.
[5] B. Denizot, G. Tanguy, F. Hindre, E. Rump, J.J. Lejeune, P. Jallet, Phosphorylcholine coating of iron oxide nanoparticles, J. Colloid Interface Sci. 209 (1999) 66–71.
[6] G.F. Goya, V. Grazu, M.R. Ibarra, Magnetic Nanoparticles for Cancer Therapy, Curr. Nanosci. 4 (1) (2008) 1–16 (16).
[7] C.C. Berry, A.S.G. Curtis, Functionalisation of magnetic nanoparticles for applications in biomedicine, J. Phys. D: Appl. Phys. 36 (2003) R198–R206.
[8] Yu-Hua Ma, Hai-Ying Peng, Rui-Xia Yang, Fang Ni, Preparation of lysine-coated magnetic Fe2O3 nanoparticles and influence on viability of A549 lung cancer cells, Asian Pac. J. Cancer Prev. 15 (20) (2014) 8981–8985.
[9] A.L. Harris, Hypoxia–a key regulatory factor in tumour growth, Nat. Rev. Cancer 2 (1) (2002) 38–47 (Review).
[10] J. Pastorek, S. Pastorekova, Hypoxia-induced carbonic anhydrase IX as a target for cancer therapy: from biology to clinical use, Semin Cancer Biol. 31 (2015) 52–64 (doi: 0.1016/j.semcancer.2014.08.002).
[11] M. Zatovicova, K. Tarabkova, E. Svastova, A. Gibadulinova, V. Mucha, L. Jakubickova, Z. Biesova, M. Rafajova, M.G. Ortova, S. Parkkila, A.K. Parkkila, A. Waheed, W.S. Sly, I. Horak, J. Pastorek, S. Pastorekova, Monoclonal antibodies generated in carbonic anhydrase IX-deficient mice recognize different domains of tumour-associated hypoxia-induced carbonic anhydrase IX, J. Immunol. Methods 282 (1–2) (2003) 117–134.
[12] M. Koneracka, P. Kopcansky, M. Antalik, M. Timko, C.N. Ramchand, D. Lobo, R.V. Mehta, R.V. Upadhyay, Immobilization of proteins and enzymes to fine magnetic particles, J. Magn. Magn. Mater. 201 (1999) 427–430.
[13] M.M. Bradford, A rapid and sensitive method for the quantitation of microgram quantities of protein utilizing the principle of protein-dye binding, Anal. Biochem. 72 (1976) 248–254.
[14] M. Koneracka, M. Muckova, V. Zavisova, N. Tomasovicova, P. Kopcansky, M. Timko, A. Jurikova, K. Csach, V. Kavecansky, Encapsulation of anticancer drug and magnetic particles in the biodegradable polymer nanospheres, J. Phys. Condens. Matter 20 (2008) (204151 (6pp).
[15] Wei-Chiang Shen, Daming Yang, Hugues J.-P. Ryser, Calorimetric determination of microgram quantities of polylysine by trypan blue precipitation, Anal. Biochem. 142 (1984) 521–524.
[16] J. Lojk, V. Bregar, M. Rajh, Cell type-specific response to high intracellular loading of polyacrylic acid-coated magnetic nanoparticles, Int. J. Nanomed. 10 (2015) 1449–1461. http://dx.doi.org/10.2147/IJN.S76134.